

# Identifying Functional Thermodynamics in Autonomous Maxwellian Ratchets

Alexander B. Boyd,<sup>1,\*</sup> Dibyendu Mandal,<sup>2,†</sup> and James P. Crutchfield<sup>1,‡</sup>

<sup>1</sup>*Complexity Sciences Center and Physics Department,*

*University of California at Davis, One Shields Avenue, Davis, CA 95616*

<sup>2</sup>*Department of Physics, University of California, Berkeley, CA 94720, U.S.A.*

(Dated: December 7, 2024)

We introduce a family of Maxwellian Demons for which correlations among information bearing degrees of freedom can be calculated exactly and in compact analytical form. This allows one to precisely determine Demon functional thermodynamic operating regimes, when previous methods either misclassify or simply fail due to approximations they invoke. These Demons are as functional as alternative candidates, behaving either as engines, lifting a mass against gravity by extracting energy from a single heat reservoir, or Landauer erasers, removing information from a sequence of binary symbols by consuming external work. In both cases, explicitly accounting for informational correlations leads to tight bounds on Demon performance, expressed as a refined Second Law of thermodynamics that relies on the Kolmogorov-Sinai entropy.

PACS numbers: 05.70.Ln 89.70.-a 05.20.-y 05.45.-a

Keywords: Maxwell’s demon, Maxwell’s refrigerator, detailed balance, entropy rate, Second Law of thermodynamics

## I. INTRODUCTION

The Second Law of thermodynamics is only statistically true: while the entropy production in any process is nonnegative on the average,  $\langle \Delta S \rangle \geq 0$ , if we wait long enough, we shall see individual events for which the entropy production is negative. This is nicely summarized in the recent fluctuation theorem for the probability of entropy production  $\Pr(\Delta S)$  [1–7]:

$$\frac{\Pr(\Delta S)}{\Pr(-\Delta S)} = e^{\Delta S} \quad , \quad (1)$$

implying that negative entropy production events are exponentially rare but not impossible. Negative entropy fluctuations were known much before this modern formulation. In fact, in 1867 J. C. Maxwell used the negative entropy fluctuations in a clever thought experiment, involving an imaginary intelligent being—later called Maxwell’s Demon—that exploits fluctuations to violate the Second Law [8, 9]. The Demon controls a small frictionless trapdoor on a partition inside a box of gas molecules to sort, without any expenditure of work, faster molecules to one side and slower ones to the other. This gives rise to a temperature gradient from an initially uniform system—a violation of the Second Law. Note that the “very observant and neat fingered” Demon’s “intelligence” is necessary; a frictionless trapdoor

connected to a spring acting as a valve, for example, cannot achieve the same feat [10].

Maxwell’s Demon posed a fundamental challenge. Either such a demon could not exist, even in principle, or the Second Law itself needed modification. A glimmer of a resolution came with L. Szilard’s reformulation of Maxwell’s Demon in terms of measurement and feedback-control of a single-molecule engine. Critically, Szilard emphasized hitherto-neglected information-theoretic aspects of the Demon’s operations [11]. Later, through the works of R. Landauer, O. Penrose, and C. Bennett, it was recognized that the Demon’s operation necessarily accumulated information and, for a repeating thermodynamic cycle, erasing this information has an entropic cost that ultimately compensates for the total amount of negative entropy production leveraged by the Demon to extract work [12–14]. In other words, with intelligence and information-processing capabilities, the Demon merely shifts the entropy burden temporarily to an information reservoir, such as its memory. The cost is repaid whenever the information reservoir becomes full and needs to be reset. This resolution is concisely summarized in Landauer’s Principle [15]: the Demon’s erasure of one bit of information at temperature  $T$  K requires at least  $k_B T \ln 2$  amount of heat dissipation, where  $k_B$  is Boltzmann’s constant. (While it does not affect the following directly, it has been known for some time that this principle is only a special case [16].)

Building on this, a modified Second Law was recently proposed that explicitly addresses information processing

\* abboyd@ucdavis.edu

† dibyendu.mandal@berkeley.edu

‡ chaos@ucdavis.edu

in a thermodynamic system [17, 18]:

$$\langle \Delta S \rangle + k_B \ln 2 \Delta H \geq 0, \quad (2)$$

where  $\Delta H$  is the information reservoir’s change over a thermodynamic cycle. This is the change in the reservoir’s “information-bearing degrees of freedom” as measured using Shannon information  $H$  [19]. These degrees of freedom are coarse-grained states of the reservoir’s microstates—the mesoscopic states that store information needed for the Demon’s thermodynamic control. Importantly for the following, this Second Law assumes *explicitly observed* Markov system dynamics [17] and quantifies this relevant information only in terms of the distribution of *instantaneous* system microstates; not, to emphasize, microstate path entropies. In short, while the system’s instantaneous distributions relax and change over time, the information reservoir itself is not allowed to build up and store memory or correlations.

Note that this framework differs from alternative approaches to the thermodynamics of information processing, including: (i) active feedback control by external means, where the thermodynamic account of the Demon’s activities tracks the mutual information between measurement outcomes and system state [20–33]; (ii) the multipartite framework where, for a set of interacting, stochastic subsystems, the Second Law is expressed via their intrinsic entropy production, correlations among them, and transfer entropy [34–37]; and (iii) steady-state models that invoke time-scale separation to identify a portion of the overall entropy production as an information current [38, 39]. A unified approach to these perspectives was attempted in Refs. [40–42].

Recently, many Maxwellian Demons have been proposed to explore plausible automated mechanisms that appeal to Eq. (2)’s modified Second Law to do useful work, by decreasing the physical entropy, at the expense of positive change in reservoir Shannon information [39, 43–49]. Paralleling the modified Second Law’s derivation and the analyses of the alternatives above, they too neglect correlations in the information-bearing components. In effect, they account for Demon information-processing by replacing the Shannon information of the components as a whole by the sum of the components’ *individual* Shannon informations. Since the latter is larger than the former [19], these analyses lead to weak bounds on Demon performance.

This Letter proposes a new Demon for which, for the first time, all correlations among system components can be explicitly accounted. This gives an exact, analytical treatment of the thermodynamically relevant Shannon information change—one that accounts for system trajectories not just information in instantaneous state

distributions. The result is a refined Second Law that subsumes Eq. (2) by properly accounting for intrinsic information processing reflected in temporal correlations via the overall dynamic’s Kolmogorov-Sinai entropy rate [50]. Notably, our Demon is just as rich as previous candidates: Depending on model parameters, it acts both as an engine, by extracting energy from a single reservoir and converting it into work, and as an information eraser, erasing Shannon information at the cost of the external input of work.

## II. INFORMATION RATCHETS

Our model consists of four components, see Fig. 1: (1) an ensemble of bits that acts as an information reservoir; (2) a weight that acts as a reservoir for storing work; (3) a thermal reservoir at temperature  $T$ ; and (4) a finite-state ratchet that mediates interactions between the three reservoirs. The bits interact with the ratchet sequentially and, depending on the incoming bit statistics and Demon parameters, the weight is either raised or lowered against gravity.

As a device that reads and processes a tape of bits, this class of ratchet model has a number of parallels that we mention now, partly to indicate possible future applications. First, one imagines a sophisticated, stateful biomolecule that scans a segment of DNA, say as a DNA polymerase does, leaving behind a modified sequence of nucleotide base-pairs [51]. Second, there is a rough similarity to a Turing machine sequentially recognizing tape symbols, updating its internal state, and taking an action by modifying the tape cell and moving its read-write head [52]. When the control logic is stochastic, this sometimes is referred to as “Brownian computing” [53, and references therein]. Finally, we are reminded of the deterministic finite-state tape processor of Ref. [54] that, despite its simplicity, indicates how undecidability can be imminent in dynamical processes. Surely there are other intriguing parallels, but these give a sense of a range of applications in which sequential information processing embedded in a thermodynamic system has relevance.

The bit ensemble is a semi-infinite sequence, broken into incoming and outgoing pieces. The ratchet runs along the sequence, interacting with each bit of the input string step by step. During each interaction at step  $N$ , the ratchet state  $X_N$  and interacting bit  $Y_N$  fluctuate between different internal joint states within  $\mathcal{X}_N \otimes \mathcal{Y}_N$ , exchanging energy with the thermal reservoir and work reservoir, and potentially changing  $Y_N$ ’s state. At the end of step  $N$ , after input bit  $Y_N$  interacts with the ratchet, it becomes the last bit  $Y'_N$  of the output string. By interacting with the ensemble of bits, transducing the

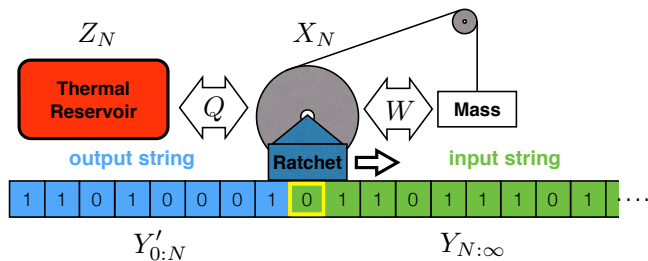


FIG. 1. Information ratchet sequentially processing a bit string: At time step  $N$ ,  $X_N$  is the random variable for the ratchet state and  $Z_N$  that for the thermal reservoir.  $Y_{N:\infty}$  is the block random variable for the input bit string and  $Y'_{0:N}$  that for the output bit string. The last bit  $Y_N$  of the input string, highlighted in yellow, interacts with the ratchet. The arrow on the right of the ratchet indicates the direction the ratchet moves along the tape as it sequentially interacts with each input bit in turn.

input string into the output string, the ratchet can convert thermal energy from the heat reservoir into work energy stored in the weight's height.

The ratchet interacts with each incoming bit for a time interval  $\tau$ , starting at the 0th bit  $Y_0$  of the input string. After  $N$  time intervals, input bit  $Y_{N-1}$  finishes interacting with the ratchet and, with the coupling removed, it is effectively “written” to the output string, becoming  $Y'_{N-1}$ . The ratchet then begins interacting with input bit  $Y_N$ . As Fig. 1 illustrates, the state of the overall system is described by the realizations of four random variables:  $X_N$  for the ratchet state,  $Y_{N:\infty}$  for the input string,  $Y'_{0:N}$  for the output string, and  $Z_N$  for the thermal reservoir. A random variable like  $X_N$  realizes elements  $x_N$  of its physical state space, denoted by alphabet  $\mathcal{X}$ , with probability  $\Pr(X_N = x_N)$ . Random variable blocks are denoted  $Y_{a:b} = Y_a Y_{a+1} \dots Y_{b-1}$ , with the last index being exclusive. In the following, we take binary alphabets for  $\mathcal{Y}$  and  $\mathcal{Y}'$ :  $y_N, y'_N \in \{0, 1\}$ . The bit ensemble is considered two joint variables  $Y'_{0:N} = Y'_0 Y'_1 \dots Y'_{N-1}$  and  $Y_{N:\infty} = Y_N Y_{N+1} \dots$  rather than one  $Y_{0:\infty}$ , so that the probability of realizing a word  $w \in \{0, 1\}^{b-a}$  in the output string is not the same as in the input string. That is, during ratchet operation typically  $\Pr(Y_{a:b} = w) \neq \Pr(Y'_{a:b} = w)$ .

The ratchet steadily transduces the input bit sequence, described by the input word distribution  $\Pr(Y_{0:\infty}) \equiv \{\Pr(Y_{0:\infty} = w)\}_{w \in \{0,1\}^\infty}$ —the probability for every semi-infinite input word—into the output string, described by the word distribution  $\Pr(Y'_{0:\infty}) \equiv \{\Pr(Y'_{0:\infty} = v)\}_{v \in \{0,1\}^\infty}$ . We assume that the word distributions we work with are stationary, meaning that  $\Pr(Y_{a:a+b}) = \Pr(Y_{0:b})$  for all nonnegative integers  $a$  and  $b$ .

A key question in working with a sequence such as  $Y_{0:\infty}$  is how random it is. One commonly turns to information

theory to provide quantitative measures: the more informative a sequence is, the more random it is. For words at a given length  $\ell$  the average amount of information in the  $Y_{0:\infty}$  sequence is given by the *Shannon block entropy* [55]:

$$\begin{aligned} H(\ell) &= H[Y_{0:\ell}] \\ &\equiv - \sum_{w \in \{0,1\}^\ell} \Pr(Y_{0:\ell} = w) \log_2 \Pr(Y_{0:\ell} = w) . \end{aligned}$$

Due to correlations in typical process sequences, the irreducible randomness per symbol is not the *single-symbol entropy*  $H(1) = H[X_0]$ . Rather, it is given by the *Kolmogorov-Sinai entropy rate* [55]:

$$h_\mu \equiv \lim_{\ell \rightarrow \infty} \frac{H(\ell)}{\ell} . \quad (3)$$

Note that these ways of monitoring information are quantitatively quite different. For large  $\ell$ ,  $h_\mu \ell \ll H(\ell)$  and, in particular, anticipating later use,  $h_\mu \leq H(1)$ . Equality between the single-symbol entropy and entropy rate is only achieved when the generating process is memoryless. Calculating the single-symbol entropy is typically quite easy, while calculating  $h_\mu$  for general processes has been known for quite some time to be difficult [56] and it remains a technical challenge [57]. The entropy rates of the output sequence and input sequence are  $h'_\mu = \lim_{\ell \rightarrow \infty} H[Y'_{0:\ell}]/\ell$  and  $h_\mu = \lim_{\ell \rightarrow \infty} H[Y_{0:\ell}]/\ell$ , respectively.

The informational properties of the input and output word distributions set bounds on energy flows in the system. Appendix A establishes one of our main results: The average work done by the ratchet is bounded above by the difference in Kolmogorov-Sinai entropy rates of the input and output processes:

$$\begin{aligned} \langle W \rangle &\leq k_B T \ln 2 (h'_\mu - h_\mu) \\ &= k_B T \ln 2 \Delta h_\mu . \end{aligned} \quad (4)$$

The preceding remarks on the relationship between entropy rate and single-symbol entropy explain why this is a substantial refinement of Eq. (2). Here, we consider the case where the ratchet is driven by a memoryless input process, meaning the input process entropy rate is the same as the single-symbol entropy:  $h_\mu = H[Y_0]$ . However, the ratchet's memory can create correlations in the output bit string, so:

$$\begin{aligned} \Delta h_\mu &= h'_\mu - H[Y_0] \\ &\leq H[Y'_0] - H[Y_0] = \Delta H . \end{aligned}$$

In this case, Eq. (4) is a stronger bound on the work done

by the ratchet—a bound that explicitly accounts for correlations within the output bit string the ratchet generates during its operation. Previously, the effect of these correlations has not been calculated. As such, this new Second Law of thermodynamics for information ratchets has important consequences for ratchet functioning and performance.

While we do not consider it here, the new Second Law also has implications for ratchet functioning when the input bits are correlated as well. Specifically, correlations in the input bits can be leveraged by the ratchet to do additional work—work that cannot be accounted for if one only considers single-symbol entropy of the input bits [58].

### III. ENERGETICS AND DYNAMICS

To predict how the ratchet interacts with the bit string and weight, we need to specify the string and ratchet energies. When not interacting with the ratchet the energies,  $E_0$  and  $E_1$ , of both bit states,  $Y = 0$  and  $Y = 1$ , are taken to be zero for symmetry and simplicity:  $E_0 = E_1 = 0$ . For simplicity, too, we say the ratchet mechanism has just two internal states  $A$  and  $B$ . When the ratchet is not interacting with bits, the two states can have different energies. We take  $E_A = 0$  and  $E_B = -\alpha k_B T$ , without loss of generality. Since the bits interact with the ratchet one at a time, we only need to specify the interaction energy of the ratchet and an individual bit. The interaction energy is zero if the bit is in the state  $Y = 0$ , regardless of the ratchet state, and it is  $-\beta k_B T$  (or  $+\beta k_B T$ ) if the bit is in state  $Y = 1$  and the ratchet is in state  $A$  (or  $B$ ). See Fig. 2 for a graphical depiction of the energy scheme under “Ratchet  $\otimes$  Bit”.

The scheme is further modified by the interaction of the weight with the ratchet and bit string. We attach the weight to the ratchet-bit system such that when the latter transitions from the  $B \otimes 0$  state to the  $A \otimes 1$  state it lifts the weight, doing a constant amount  $w k_B T$  of work. As a result, the energy of the composite system—demon, interacting bit, and weight—increases by  $w k_B T$  whenever the transition  $B \otimes 0 \rightarrow A \otimes 1$  takes place, the required energy being extracted from the heat reservoir  $Z_N$ . The rightmost part of Fig. 2 indicates this by raising the energy level of  $A \otimes 1$  by  $w k_B T$  compared to its previous value. Since the transitions between  $A \otimes 1$  and  $B \otimes 1$  do not involve the weight, their relative energy difference remains unaffected. An increase in the energy of  $A \otimes 1$  by  $w k_B T$  therefore implies the same increase in the energy of  $B \otimes 1$ . Again, see Fig. 2 for the energy scheme under “Ratchet  $\otimes$  Bit  $\otimes$  Weight”.

The time evolution over the joint state space of the

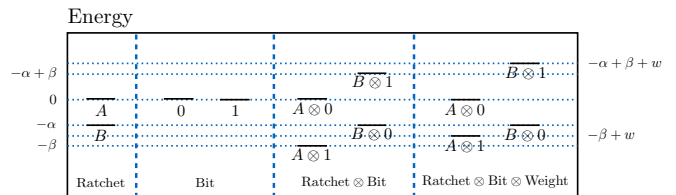


FIG. 2. Energy levels of the Demon states, interacting bits, their joint system, and their joint system with a weight in units of  $[k_B T]$ .

ratchet, last bit of the input string, and weight is governed by a Markov dynamic, specified by state-transition matrix  $M$ . If, at the beginning of the  $N$ th interaction interval at time  $t = \tau(N - 1) + 0^+$ , the ratchet is in state  $X_N = x_N$  and the input bit is in state  $Y_N = y_N$ , then let  $M_{x_N \otimes y_N \rightarrow x_{N+1} \otimes y'_N}$  be the probability  $\Pr(x_{N+1}, y'_N | x_N, y_N)$  that the ratchet is in state  $X_N = x_{N+1}$  and the bit is in state  $Y_N = y'_N$  at the end of the interaction interval  $t = \tau(N - 1) + \tau^-$ .  $X_N$  and  $Y_N$  at the end of the  $N$ th interaction interval become  $X_{N+1}$  and  $Y'_N$  respectively at the beginning of the  $N + 1$ th interaction interval. Since we assume the system is thermalized with a bath at temperature  $T$ , the ratchet dynamics obey detailed balance. And so, transition rates are governed by the energy differences between joint states:

$$\frac{M_{x_N \otimes y_N \rightarrow x_{N+1} \otimes y'_N}}{M_{x_{N+1} \otimes y'_N \rightarrow x_N \otimes y_N}} = e^{(E_{x_{N+1} \otimes y'_N} - E_{x_N \otimes y_N}) / k_B T}.$$

There is substantial flexibility in constructing a detailed-balanced Markov dynamic for the ratchet, interaction bit, and weight. Consistent with our theme of simplicity, we choose one that has only six allowed transitions:  $A \otimes 0 \leftrightarrow B \otimes 0$ ,  $A \otimes 1 \leftrightarrow B \otimes 1$ , and  $A \otimes 1 \leftrightarrow B \otimes 0$ . Such a model is convenient to consider, since it can be described by just two transition probabilities  $0 \leq p \leq 1$  and  $0 \leq q \leq 1$ , as shown in Fig. 3.

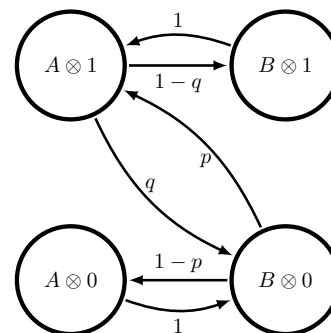


FIG. 3. The Markovian, detailed-balance dynamic over the joint states of the ratchet and interacting bit.

The Markov transition matrix for this system is given by:

$$M = \begin{bmatrix} 0 & 1-p & 0 & 0 \\ 1 & 0 & q & 0 \\ 0 & p & 0 & 1 \\ 0 & 0 & 1-q & 0 \end{bmatrix}.$$

This allows us to calculate the state distribution  $\mathbf{p}((N-1)\tau + \tau^-)$  at the end of the  $N$ th interaction interval from the state distribution  $\mathbf{p}((N-1)\tau + 0^+)$  at the interval's beginning via:

$$\mathbf{p}((N-1)\tau + \tau^-) = M\mathbf{p}((N-1)\tau + 0^+),$$

where the probability vector is indexed  $\mathbf{p} = (\Pr(A \otimes 0), \Pr(B \otimes 0), \Pr(A \otimes 1), \Pr(B \otimes 1))^\top$ . To satisfy detailed balance, we find that  $\alpha$ ,  $\beta$ , and  $w$  should be:

$$\alpha = -\ln(1-p), \quad (5)$$

$$\beta = -\frac{1}{2} \ln[(1-p)(1-q)], \quad \text{and} \quad (6)$$

$$w = \ln\left(\frac{q\sqrt{1-p}}{p\sqrt{1-q}}\right). \quad (7)$$

(Appendix B details the relationships between the transitions probabilities and energy levels.)

This simple model is particularly useful since, as we show shortly, it captures the full range of thermodynamic functionality familiar from previous models and, more importantly, it makes it possible to exactly calculate informational properties of the output string analytically.

Now that we know how the ratchet interacts with the bit string and weight, we need to characterize the input string to predict the energy flow through the ratchet. As in the ratchet models of Refs. [43, 47], we consider an input generated by a biased coin— $\Pr(Y_N = 0) = b$  at each  $N$ —which has no correlations between successive bits. For this input, the steady state distributions at the beginning and end of the interaction interval  $\tau$  are:

$$\mathbf{p}^s(0^+) = \frac{1}{2} \begin{bmatrix} b \\ b \\ 1-b \\ 1-b \end{bmatrix} \quad \text{and} \\ \mathbf{p}^s(\tau^-) = \frac{1}{2} \begin{bmatrix} b(1-p) \\ b+q-bq \\ bp+1-b \\ (1-b)(1-q) \end{bmatrix}. \quad (8)$$

These distributions are needed to calculate the work done by the ratchet.

To calculate net extracted work by the ratchet we need to consider three work-exchange steps for each interac-

tion interval: (1) when the ratchet gets attached to a new bit, to account for their interaction energy; (2) when the joint transitions  $B \otimes 0 \leftrightarrow A \otimes 1$  take place, to account for the raising or lowering of the weight; and (3) when the ratchet detaches itself from the old bit, again, to account for their nonzero interaction energy. We refer to these incremental works as  $W_1$ ,  $W_2$ , and  $W_3$ , respectively.

Consider the work  $W_1$ . If the new bit is in state 0, from Fig. 2 we see that there is no change in the energy of the joint system of the ratchet and the bit. However, if the new bit is 1 and the initial state of the ratchet is  $A$ , energy of the ratchet-bit joint system decreases from 0 to  $-\beta$ . The corresponding energy is gained as work by the mechanism that makes the ratchet move past the tape of bits. Similarly, if the new bit is 1 and the initial state of the ratchet is  $B$ , there is an increase in the joint state energy by  $\beta$ ; this amount of energy is now taken away from the driving mechanism of the ratchet. In the steady state, the average work gain  $\langle W_1 \rangle$  is then obtained from the average decrease in energy of the joint (ratchet-bit) system:

$$\begin{aligned} \langle W_1 \rangle &= - \sum_{\substack{x \in \{A,B\} \\ y \in \{0,1\}}} p_{x \otimes y}^s(0^+) (E_{x \otimes y} - E_x - E_y) \\ &= 0, \end{aligned}$$

where we used the probabilities in Eq. (8) and Fig. 2's energies.

By a similar argument, the average work  $\langle W_3 \rangle$  is equal to the average decrease in the energy of the joint system on the departure of the ratchet, given by:

$$\langle W_3 \rangle = -\frac{k_B T}{2} \beta [q + b(p-q)].$$

Note that the cost of moving the Demon on the bit string (or moving the string past a stationary Demon) is accounted for in works  $W_1$  and  $W_3$ .

Work  $W_2$  is associated with raising and lowering of the weight depicted in Fig. 1. Since transitions  $B \otimes 0 \rightarrow A \otimes 1$  raise the weight to give work  $k_B T w$  and reverse transitions  $B \otimes 0 \leftarrow A \otimes 1$  lower the weight consuming equal amount of work, the average work gain  $\langle W_2 \rangle$  must be  $k_B T w$  times the net probability transition along the former direction, which is  $[T_{B \otimes 0 \rightarrow A \otimes 1} p_{B \otimes 0}^s(0^+) - T_{A \otimes 1 \rightarrow B \otimes 0} p_{A \otimes 1}^s(0^+)]$ . This leads to the following expression:

$$\langle W_2 \rangle = \frac{k_B T w}{2} [-q + b(p+q)],$$

where we used the probabilities in Eq. (8).

The total work supplied by the ratchet and a bit is

their sum:

$$\begin{aligned} \langle W \rangle &= \langle W_1 \rangle + \langle W_2 \rangle + \langle W_3 \rangle \\ &= \frac{k_B T}{2} [(pb - q + qb) \ln \left( \frac{q}{p} \right) \\ &\quad + (1 - b)q \ln(1 - q) + pb \ln(1 - p)] . \end{aligned} \quad (9)$$

Note that we considered the total amount of work that can be gained by the system, not just that obtained by raising the weight. Why? As we shall see in Sec. V, the former is the thermodynamically more relevant quantity. A similar energetic scheme that incorporates the effects of interaction has also been discussed in Ref. [49].

In this way, we exactly calculated the work term in Eq. (4). We still need to calculate the entropy rate of the output and input strings to validate the proposed Second Law. For this, we introduce an information-theoretic formalism to monitor processing of the bit strings by the ratchet.

#### IV. INFORMATION

To analytically calculate the input and output entropy rates, we consider how the strings are generated. A natural way to incorporate temporal correlations in the input string is to model its generator by a finite-state hidden Markov model (HMM), since HMMs are strictly more powerful than Markov chains in the sense that finite-state HMMs can generate all processes produced by Markov chains, but the reverse is not true. For example, there are processes generated by finite HMMs that cannot be by any finite-state Markov chain. In short, HMMs give a compact representations for a wider range of memoryful processes.

Consider possible input strings to the ratchet. With or without correlations between bits, they can be described by an HMM generator with a finite set of, say,  $K$  states and a set of two symbol-labeled transition matrices  $T^{(0)}$  and  $T^{(1)}$ , where:

$$T_{s_N \rightarrow s_{N+1}}^{(y_N)} = \Pr(Y_N = y_N, S_{N+1} = s_{N+1} | S_N = s_N)$$

is the probability of outputting  $y_N$  for the  $N$ th bit of the input string and transitioning to internal state  $s_{N+1}$  given that the HMM was in state  $s_N$ .

When it comes to the output string, in contrast, we have no choice. We are forced to use HMMs. Since the current input bit state  $Y_N$  and ratchet state  $X_N$  are not explicitly captured in the current output bit state  $Y'_N$ ,  $Y_N$  and  $X_N$  are hidden variables. As we noted before, calculating HMM entropy rates is a known challenging problem [56, 57]. Much of the difficulty stems from the

fact that in HMM-generated processes the effects of internal states are only indirectly observed and, even then, appear only over long output sequences.

We can circumvent this difficulty by using *unifilar* HMMs, in which the current state and generated symbol uniquely determine the next state. This is a key technical contribution here since for unifilar HMMs the entropy rate is exactly calculable, as we now explain. Unifilar HMMs internal states are a causal partitioning of the past, meaning that every past  $w$  maps to a particular state through some function  $f$  and so:

$$\Pr(Y_N = y_N | Y_{0:N} = w) = \Pr(Y_N = y_N | S_N = f(w)) .$$

As a consequence, the entropy rate  $h_\mu$  in its block-entropy form (Eq. (3)) can be re-expressed in terms of the transition matrices. First, recall the alternative, equivalent form for entropy rate:  $h_\mu = \lim_{N \rightarrow \infty} H[Y_N | Y_{0:N}]$ . Second, since  $S_N$  captures all the dependence of  $Y_N$  on the past,  $h_\mu = \lim_{N \rightarrow \infty} H[Y_N | S_N]$ . This finally leads to a closed-form for the entropy rate [55]:

$$\begin{aligned} h_\mu &= \lim_{N \rightarrow \infty} H[Y_N | S_N] \\ &= - \sum_{y_N, s_N, s_{N+1}} \pi_{s_N} T_{s_N \rightarrow s_{N+1}}^{(y_N)} \log_2 T_{s_N \rightarrow s_{N+1}}^{(y_N)} , \end{aligned} \quad (10)$$

where  $\pi$  is the stationary distribution over the unifilar HMM's states.

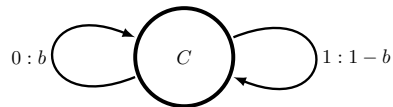


FIG. 4. Biased coin input string as a unifilar hidden Markov model with bias  $\Pr(Y = 0) = b$ .

Let's now put these observations to work. Here, we assume the ratchet's input string was generated by a memoryless biased coin. Figure 4 shows its (minimal-size) unifilar HMM. The single internal state  $C$  implies that the process is memoryless and the bits are uncorrelated. The HMM's symbol-labeled  $(1 \times 1)$  transition matrices are  $T^{(0)} = [b]$  and  $T^{(1)} = [1 - b]$ . The transition from state  $C$  to itself labeled  $0 : b$  means that if the system is in state  $C$ , then it transitions to state  $C$  and outputs  $Y = 0$  with probability  $b$ . Since this model is unifilar, we can calculate the input-string entropy rate from Eq. (10) and see that it is the single-symbol entropy of bias  $b$ :

$$\begin{aligned} h_\mu &= H(b) \\ &\equiv -b \log_2 b - (1 - b) \log_2 (1 - b) , \end{aligned}$$

where  $H(b)$  is the (base 2) binary entropy function [19].

The more challenging part of our overall analysis is to determine the entropy rate of the output string. Even if the input is uncorrelated, it's possible that the ratchet creates temporal correlations in the output string. (Indeed, these correlations reflect the ratchet's operation and so its thermodynamic behavior, as we shall see below.) To calculate the effect of these correlations, we need a generating unifilar HMM for the output process—a process produced by the ratchet being driven by the input.

When discussing the ratchet energetics, there was a Markov dynamic  $M$  over the ratchet-bit joint state space. Here, it is now controlled by bits from the input string and writes the result of the thermal interaction with the ratchet to the output string. In this way,  $M$  becomes an input-output machine or *transducer* [59]. In fact, this transducer is a communication channel in the sense of Shannon [60] that communicates the input bit sequence to the output bit sequence. However, it is a channel with memory. Its internal states correspond to the ratchet's states. To work with  $M$ , we rewrite it componentwise as:

$$M_{x_N \rightarrow x_{N+1}}^{(y'_N | y_N)} = M_{x_N \otimes y_N \rightarrow x_{N+1} \otimes y'_N}$$

to evoke its re-tooled operation. The probability of generating bit  $y'_N$  and transitioning to ratchet state  $x_{N+1}$ , given that the input bit is  $y_N$  and the ratchet is in state  $x_N$ , is:

$$M_{x_N \rightarrow x_{N+1}}^{(y'_N | y_N)} = \Pr(Y'_N = y'_N, X_{N+1} = x_{N+1} | Y_N = y_N, X_N = x_N).$$

This allows us to exactly calculate the symbol-labeled transition matrices,  $T^{(0)}$  and  $T^{(1)}$ , of the HMM that generates the output string:

$$T'_{s_N \otimes x_N \rightarrow s_{N+1} \otimes x_{N+1}}^{(y'_N)} = \sum_{y_N} M_{x_N \rightarrow x_{N+1}}^{(y'_N | y_N)} T_{s_N \rightarrow s_{N+1}}^{(y_N)}.$$

The joint states of the ratchet and the internal states of the input process are the internal states of the output HMM, with  $x_N, x_{N+1} \in \{A, B\}$  and  $s_N, s_{N+1} \in \{C\}$  in the present case. This approach is a powerful tool for directly analyzing informational properties of the output process.

By adopting the transducer perspective, it is possible to find HMMs for the output processes of previous ratchet models, such as in Refs. [43, 47]. However, their generating HMMs are highly nonunifilar, meaning that knowing the current internal state and output allows for many alternative internal-state paths. And, this precludes writing down closed-form expressions for informational quantities, as we do here. Said simply, the essential problem is

that those models build in too many transitions. Ameliorating this constraint led to the Markov dynamic shown in Fig. 3 with two ratchet states and sparse transitions. Although this ratchet's behavior cannot be produced by a rate equation, due to the limited transitions, it respects detailed balance.

Figure 5 shows our two-state ratchet's transducer. As noted above, it's internal states are the ratchet states. Each transition is labeled  $y'|y : p$ , where  $y'$  is the output, conditioned on an input  $y$ , with probability  $p$ .

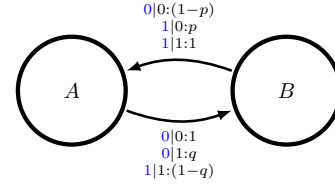


FIG. 5. The Maxwellian ratchet's transducer.

We can drive this ratchet (transducer) with any input, but for comparison with previous work, we drive it with the memoryless biased coin process just introduced and shown in Fig. 4. The resulting unifilar HMM for the output string is shown in Fig. 6. The corresponding symbol-labeled transition matrices are:

$$T^{(0)} = \begin{bmatrix} 0 & (1-p)b \\ b + q(1-b) & 0 \end{bmatrix}, \text{ and} \quad (11)$$

$$T^{(1)} = \begin{bmatrix} 0 & 1 - (1-p)b \\ (1-q)(1-b) & 0 \end{bmatrix}. \quad (12)$$

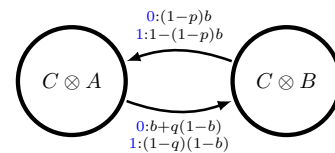


FIG. 6. Unifilar HMM for the output string generated by the ratchet driven by a coin with bias  $b$ .

Using these we can complete our validation of the proposed Second Law, by exactly calculating the entropy rate of the output string. We find:

$$\begin{aligned} h'_\mu &= \lim_{N \rightarrow \infty} H[Y'_N | Y'_{0:N}] \\ &= \lim_{N \rightarrow \infty} H[Y'_N | S_N] \\ &= \frac{H[b(1-p)]}{2} + \frac{H[(1-b)(1-q)]}{2}. \end{aligned}$$

We note that this is less than or equal to the (uncondi-

tioned) single-symbol entropy for the output process:

$$\begin{aligned} h'_\mu &\leq H[Y'_0] \\ &= H((b(1-p) + (1-b)(1-q))/2) . \end{aligned}$$

Any difference between  $h'_\mu$  and single-symbol entropy  $H(\ell = 1)$  indicates correlations that the ratchet created in the output from the uncorrelated input string. In short, the entropy rate gives a more accurate picture of how information is flowing between bit strings and the heat bath. And, as we now demonstrate, the entropy rate leads to correctly identifying important classes of ratchet thermodynamic functioning—functionality the single-symbol entropy misses.

## V. THERMODYNAMIC FUNCTIONALITY

Let's step back to review and set context for exploring the ratchet's thermodynamic functionality as we vary its parameters. Our main results are analytical, provided in closed-form. First, we derived a modified version of the Second Law of thermodynamics for information ratchets in terms of the difference between the Kolmogorov-Sinai entropy rates of the input and output strings:

$$\langle W \rangle \leq k_B T \ln 2 \Delta h_\mu , \quad (13)$$

where  $\Delta h_\mu = h'_\mu - h_\mu$ . The improvement here takes into account correlations within the input string and those in the output string actively generated by the ratchet during its operation. From basic information-theoretic identities we know this new bound is stricter for memoryless inputs than previous relations [61] that ignored correlations. However, by how much? And, this brings us to our second main result. We gave analytic expressions for both the input and output entropy rates and the work done by the Demon. Now, we are ready to test that the bound is satisfied and to see how much stricter it is than earlier approximations.

We find diverse thermodynamic behaviors as shown in Figure 7, which describes ratchet thermodynamic function at input bias  $b = 0.9$ . We note that there are analogous behaviors for all values of input bias. We identified three possible behaviors for the ratchet: *Engine*, *Dud*, and *Eraser*. Nowhere does the ratchet violate the rule  $\langle W \rangle \leq k_B T \ln 2 \Delta h_\mu$ . The engine regime is defined by  $(p, q)$  for which  $k_B T \ln 2 \Delta h_\mu \geq \langle W \rangle > 0$  since work is positive. This is the only condition for which the ratchet extracts work. The eraser regime is defined by  $0 > k_B T \ln 2 \Delta h_\mu \geq \langle W \rangle$ , meaning that work is extracted from the work reservoir while the uncertainty in the bit string decreases. In the dud regime, those  $(p, q)$  for which

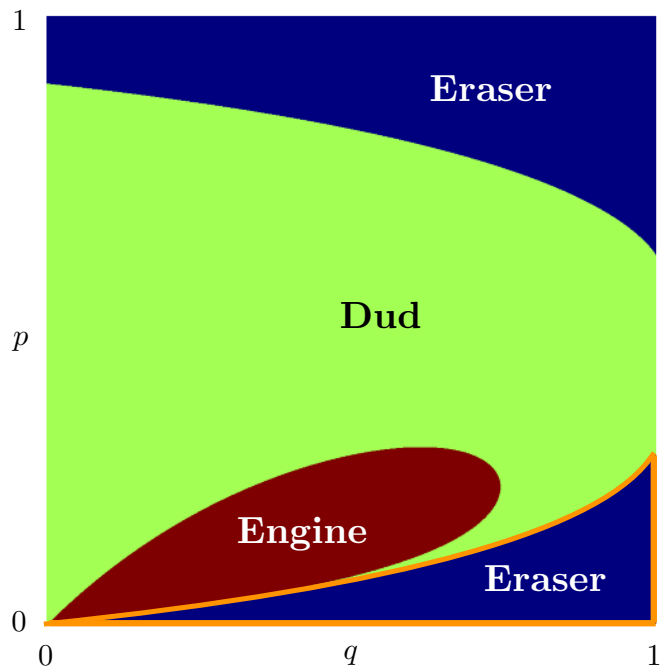


FIG. 7. Information ratchet thermodynamic functionality at input bias  $b = 0.9$ : Engine:  $(p, q)$  such that  $0 < \langle W \rangle \leq k_B T \ln 2 \Delta h_\mu$ . Eraser:  $(p, q)$  such that  $\langle W \rangle \leq k_B T \ln 2 \Delta h_\mu < 0$ . Dud:  $(p, q)$  such that  $\langle W \rangle \leq 0 \leq k_B T \ln 2 \Delta h_\mu$ .

$k_B T \ln 2 \Delta h_\mu \geq 0 \geq \langle W \rangle$ , the ratchet is neither able to erase information nor is it able to do useful work.

These are the same behavior types reported by Ref. [43], except that we have stronger bounds on the work now with  $k_B T \ln 2 \Delta h_\mu$ , compared to the single-symbol entropy approximation. The stricter bound gives deeper insight into ratchet functionality. To give a concrete comparison, Fig. 8 plots the single-symbol entropy difference  $\Delta H(1)$  and the entropy rate difference  $\Delta h_\mu$ , with a flat surface identifying zero entropy change, for all  $p$  and  $q$  and at  $b = 0.9$ .

The blue  $\Delta H(1)$  surface lies above the red  $\Delta h_\mu$  surface for all parameters, confirming that the single-symbol entropy difference is always greater than the entropy rate difference. It should also be noted for this choice of input bias  $b$  and for larger  $p$ ,  $\Delta H(1)$  and  $\Delta h_\mu$  are close, but they diverge for smaller  $p$ . They diverge so much, however, that looking only at single-symbol entropy approximation misses an entire low- $p$  region, highlighted in orange in Fig. 8 and 7, where  $\Delta h_\mu$  dips below zero and the ratchet functions as eraser.

The orange-outlined low- $p$  erasure region is particularly interesting, since it lies very close to the region where ratchet functions as an engine, as shown in Fig. 7. As one approaches  $(p, q) = (0, 0)$  the eraser and engine regions become arbitrarily close in parameter space. This is a functionally meaningful region, since the device

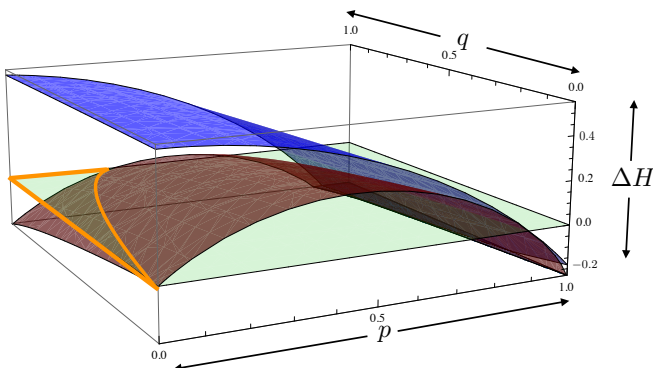


FIG. 8. Exact entropy rate difference  $\Delta h_\mu$  (red) is a much stricter bound on work than the difference in single-symbol entropy  $\Delta H(1)$  (blue). The zero surface (light green) highlights where both entropies are greater than zero and so is an aid to identifying functionalities.

can be easily and efficiently switched between distinct modalities—an eraser or an engine.

In contrast, without knowing the exact entropy rate, it appears that the engine region of the ratchet’s parameter space is isolated from the eraser region by a large dud region and that the ratchet is not tunable. Thus, knowing the correlations between bits in the output string allows one to predict additional functionality that otherwise is obscured when one only considers the single-symbol entropy of the output string.

As alluded to above, we can also consider structured input strings generated by memoryful processes, unlike the memoryless biased coin. While correlations in the output string are relevant to the energetic behavior of this ratchet, it turns out that input string correlations are not. The work done by the ratchet depends only on the input’s single-symbol bias  $b$ . That said, elsewhere we will explore more intelligent ratchets that take advantage of input string correlations to do additional work.

## CONCLUSION

Thermodynamic systems that include information reservoirs as well as thermal and work reservoirs are an area of growing interest, driven in many cases by biomolecular chemistry and nanoscale physics and engineering. With the ability to manipulate thermal systems on energy scales closer and closer to the level of thermal fluctuations  $k_B T$ , information becomes critical to the flow of energy. Our model of a ratchet and a bit string as the information reservoir is very flexible and our methods showed how to analyze a broad class of such controlled thermodynamic systems using a much tighter Second-Law bound based on the control system’s

Kolmogorov-Sinai entropy.

Though its perspective and methods were not explicitly highlighted, *computational mechanics* [62] played a critical role in the foregoing analyses, from its focus on structure and calculating all system component correlations to the technical emphasis on unifilarity in Demon models. Its full impact was not fully explicated here and is left to sequels and sister works. Two complementary computational mechanics analyses of information engines come to mind, in this light. The first is Ref. [16]’s demonstration that the chaotic instability in Szilard’s Engine, reconceived as a deterministic dynamical system, is key to its ability to extract heat from a reservoir. Another is the thorough-going extension of fluctuation relations to show how intelligent agents can harvest energy when synchronizing to the fluctuations from a structured environment [58].

This is to say, in effect, the foregoing showed that computational mechanics is a natural framework for analyzing a ratchet interacting with an information reservoir to extract work from a thermal bath. The input and output strings that compose the information reservoir are best described by unifilar HMM generators, since they allow for exact calculation of any informational property of the strings, most importantly the entropy rate. In fact, the control system components are the  $\epsilon$ -machines and  $\epsilon$ -transducers of computational mechanics [59, 62]. By allowing one to exactly calculate the asymptotic entropy rate, we identified more functionality in the effective thermodynamic  $\epsilon$ -transducers than previous methods can reveal. One immediate consequence is that our ratchet is easily tunable between an eraser and an engine—a functionality that suggests useful future engineering applications. The ratchet itself was naturally represented by an  $\epsilon$ -transducer mapping an input HMM to an output HMM. The form of this transducer is exactly calculable from the detailed balanced dynamic over the ratchet and bits. Here, we only considered memoryless biased coin inputs, but the formalism has the capacity to consider the importance of correlations in the input string as well as the output string, suggesting an even wider range of functional thermodynamics.

## ACKNOWLEDGMENTS

We thank M. DeWeese for useful conversations. As an External Faculty member, JPC thanks the Santa Fe Institute for its hospitality during visits. This work was supported in part by the U. S. Army Research Laboratory and the U. S. Army Research Office under contracts W911NF-13-1-0390 and W911NF-12-1-0234.

## Appendix A: A New Second Law

The Second Law of thermodynamics states that the total change in entropy of an isolated system has to be non-negative over any time interval. By considering a system composed of a thermal reservoir, information reservoir, and ratchet, here we derive an analogue in terms of rates, rather than total entropy changes.

Due to the Second Law, we insist that the change in thermodynamic entropy of the closed system is positive for any number  $N$  of time steps. If  $X$  is the ratchet,  $Y$  is the bit string, and  $Z$  is the heat bath, this assumption translates to:

$$\Delta S[X, Y, Z] \geq 0 .$$

Note that we do not include a term for the weight, because it doesn't contribute to the thermodynamic entropy. Expressing the thermodynamic entropy  $S$  in terms the Shannon entropy of the random variables  $S[X, Y, Z] = k_B \ln 2 H[X, Y, Z]$ , we have the condition:

$$\Delta H[X, Y, Z] \geq 0 .$$

To be more precise, this is true for any number of time steps  $N$ . If we have our system  $X$ , we express the random variable for the system at time step  $N$  by  $X_N$ . The information reservoir  $Y$  is a semi-infinite string. At time zero, the string is composed entirely of the bits of the input process, for which the random variable is denoted  $Y_{0:\infty}$ . The ratchet transduces these inputs, starting with  $Y_0$  and generating the output bit string, the entirety of which is expressed by the random variable  $Y'_{0:\infty}$ . At the  $N$ th time step, the first  $N$  bits of the input have been converted into the first  $N$  bits of the output, so the random variable for the input-output bit string is  $Y_{N:\infty} \otimes Y'_{0:N}$ . Thus, the change in entropy from the initial time to the  $N$ th time step is:

$$\begin{aligned} \Delta H_N[X, Y, Z] &= H[X_N, Y_{N:\infty}, Y'_{0:N}, Z_N] \\ &\quad - H[X_0, Y_{0:\infty}, Z_0] \\ &= H[X_N, Y_{N:\infty}, Y'_{0:N}] + H[Z_N] \\ &\quad - I[X_N, Y_{N:\infty}, Y'_{0:N}; Z_N] \\ &\quad - H[X_0, Y_{0:\infty}] - H[Z_0] \\ &\quad + I[X_0, Y_{0:\infty}; Z_0] . \end{aligned}$$

Note that the internal states of an infinite heat bath do not correlate with the environment, since they have no memory of the environment. This means the mutual information of the thermal reservoir  $Z$  with the bit string

$Y$  and ratchet  $X$  vanish. This gives:

$$\begin{aligned} \Delta H_N[X, Y, Z] &= H[X_N, Y_{N:\infty}, Y'_{0:N}] + H[Z_N] \\ &\quad - H[X_0, Y_{0:\infty}] - H[Z_0] \\ &= H[X_N] - H[X_0] + H[Z_N] - H[Z_0] \\ &\quad + H[Y_{N:\infty}, Y'_{0:N}] - H[Y_{0:\infty}] \\ &\quad - I[X_N; Y_{N:\infty}, Y'_{0:N}] \\ &\quad + I[X_0; Y_{0:\infty}] . \end{aligned}$$

The change in thermal bath entropy can be expressed  $\Delta H[Z] = H[Z_N] - H[Z_0] = Q/k_B T \ln 2$ , where  $Q$  is the heat energy that flows into the thermal bath.

Since the change in Shannon entropy of the heat reservoir, ratchet, and bit string must be greater than zero, the average change in entropy per time step  $\langle \Delta H \rangle_N = \Delta H_N[X, Y, Z]/N$  also has to be greater than zero. This is true for all  $N$ , thus:

$$\begin{aligned} \lim_{N \rightarrow \infty} \langle \Delta H \rangle_N &= \lim_{N \rightarrow \infty} \frac{\Delta H_N[X, Y, Z]}{N} \\ &\geq 0 . \end{aligned}$$

$H[X]$  is bounded by the number of states in the ratchet; so, for finite ratchets,  $\lim_{N \rightarrow \infty} H[X]/N = 0$ . Similarly,  $I[X_N; Y_{N:\infty}, Y'_{0:N}]$  and  $I[X_0; Y_{0:\infty}]$  are bounded by the number of ratchet states, so those terms vanish in the limit of infinite  $N$ . Thus, the previous expression simplifies to:

$$\begin{aligned} \lim_{N \rightarrow \infty} \langle \Delta H \rangle_N &= \lim_{N \rightarrow \infty} \left( \frac{Q}{N k_B T \ln 2} \right. \\ &\quad \left. + \frac{H[Y_{N:\infty}, Y'_{0:N}]}{N} - \frac{H[Y_{0:\infty}]}{N} \right) \\ &= \frac{\langle Q \rangle}{k_B T \ln 2} + \lim_{N \rightarrow \infty} \frac{H[Y'_{0:N}]}{N} \\ &\quad + \lim_{N \rightarrow \infty} \frac{H[Y_{N:\infty}] - H[Y_{0:\infty}]}{N} \\ &\quad - \lim_{N \rightarrow \infty} \frac{I[Y_{N:\infty}; Y'_{0:N}]}{N} , \end{aligned}$$

where  $\langle Q \rangle$  is the average heat dissipated in one time step.  $\lim_{N \rightarrow \infty} H[Y'_{0:N}]/N$  is the output process's entropy rate  $h'_\mu$ . While  $\lim_{N \rightarrow \infty} (H[Y_{N:\infty}] - H[Y_{0:\infty}])/N$  looks unfamiliar, it is actually the negative entropy rate of the input process  $h_\mu$ , so we find that:

$$\frac{\langle Q \rangle}{k_B T \ln 2} + h'_\mu - h_\mu \geq \lim_{N \rightarrow \infty} \frac{I[Y_{N:\infty}; Y'_{0:N}]}{N} .$$

To understand the righthand side, note that  $Y'_{0:N}$  is generated from  $Y_{0:N}$ , so it is independent of  $Y_{N:\infty}$  conditioned on  $Y_{0:N}$ . Essentially,  $Y_{0:N}$  causally shields  $Y'_{0:N}$

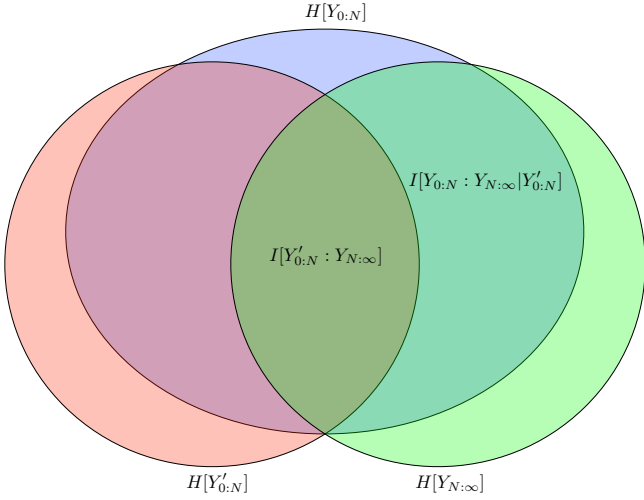


FIG. 9. The  $N$  most recent variables of the input process shield the  $N$  variables of output from the rest of the input variables.

from  $Y_{N:\infty}$ , as shown in Fig 9. This means:

$$I[Y_{N:\infty}; Y'_{0:N}] = I[Y_{N:\infty}; Y_{0:N}] - I[Y_{N:\infty}; Y_{0:N} | Y'_{0:N}].$$

This, in turn, gives:  $I[Y_{N:\infty}; Y_{0:N}] \geq I[Y_{N:\infty}; Y'_{0:N}] \geq 0$ . Thus:

$$\lim_{N \rightarrow \infty} I[Y_{N:\infty}; Y'_{0:N}] \leq \lim_{N \rightarrow \infty} I[Y_{N:\infty}; Y_{0:N}] = \mathbf{E},$$

where  $\mathbf{E}$  is the input process's excess entropy [55]. If the input is generated by a finite-state model, then  $\mathbf{E}$  is finite, meaning:

$$\lim_{N \rightarrow \infty} \frac{I[Y_{N:\infty}; Y'_{0:N}]}{N} \leq \lim_{N \rightarrow \infty} \frac{\mathbf{E}}{N} = 0.$$

For inputs generated by finite-state processes, we have:

$$\langle Q \rangle + k_B T \ln 2 (h'_\mu - h_\mu) = \langle Q \rangle + k_B T \ln 2 \Delta h_\mu \geq 0.$$

It should also be noted that for an input process with infinite states, it is possible that this is bounded below by a quantity greater than zero. Since the ratchet can only hold a finite amount of energy, for long times the average work must be opposite the average heat dissipated, and

so:

$$\langle W \rangle \leq k_B T \ln 2 \Delta h_\mu,$$

our new Second Law.

## Appendix B: Designing Ratchet Energetics

Figure 3 is one of the simplest information transducers for which the outcomes are unifilar for uncorrelated inputs, resulting in the fact that the correlations in the outgoing bits can be explicitly calculated. As this calculation was a primary motivation in our work, we introduced the model in Fig. 3 first and, only then, introduced the associated energetic and thermodynamic quantities, as in Fig. 2. The introduction of energetic and thermodynamic quantities for an abstract transducer (as in Fig. 3), however, is not trivial. Given a transducer topology (such as the reverse “Z” shape of the current model), there are multiple possible energy schemes of which only a fraction are consistent with all possible values of the associated transition probabilities. However, more than one scheme is generally possible.

To show that only a fraction of all possible energetic schemes are consistent with all possible parameter values, consider the case where the interaction energy between the ratchet and a bit is zero, as in Ref. [43]. In our model, this implies  $\beta = 0$ , or equivalently,  $p = q = 0$  (from Eq. (6)). In other words, we cannot describe our model, valid for all values  $0 < p, q < 1$ , by the energy scheme in Fig. 2 with  $\beta = 0$ . This is despite the fact that we have two other independent parameters  $\alpha$  and  $w$ .

To show that, nonetheless, more than one scheme is possible, imagine the case with  $\alpha = \beta = 0$ . Instead of just one mass, consider three masses such that, whenever the transitions  $A \otimes 0 \rightarrow B \otimes 0$ ,  $B \otimes 0 \rightarrow A \otimes 1$ , and  $A \otimes 1 \rightarrow B \otimes 1$  take place, we get works  $k_B T \widetilde{W}_1$ ,  $k_B T \widetilde{W}_2$ , and  $k_B T \widetilde{W}_3$ , respectively. We lose the corresponding amounts of work for the reverse transitions. This picture is consistent with the abstract model of Fig. 3 if the following requirements of detailed balance are satisfied:

$$\frac{1}{1-p} = \frac{M_{A \otimes 0 \rightarrow B \otimes 0}}{M_{B \otimes 0 \rightarrow A \otimes 0}} = e^{-\widetilde{W}_1}, \quad (\text{B1})$$

$$\frac{p}{q} = \frac{M_{B \otimes 0 \rightarrow A \otimes 1}}{M_{A \otimes 1 \rightarrow B \otimes 0}} = e^{-\widetilde{W}_2}, \quad \text{and} \quad (\text{B2})$$

$$1-q = \frac{M_{A \otimes 1 \rightarrow B \otimes 1}}{M_{B \otimes 1 \rightarrow A \otimes 1}} = e^{-\widetilde{W}_3}. \quad (\text{B3})$$

Existence of such an alternative scheme illustrates the fact that given the abstract model of Fig. 3, there is more than one possible consistent energy scheme. We suggest that this will allow for future engineering flexibility.

- 
- [1] D. J. Evans, E. G. D. Cohen, and G. P. Morriss. Probability of second law violations in shearing steady flows. *Phys. Rev. Lett.*, 71:2401–2404, 1993.
- [2] D. J. Evans and D. J. Searles. Equilibrium microstates which generate second law violating steady states. *Phys. Rev. E*, 50:1645, 1994.
- [3] G. Gallavotti and E. G. D. Cohen. Dynamical ensembles in nonequilibrium statistical mechanics. *Phys. Rev. Lett.*, 74:2694–2697, 1995.
- [4] J. Kurchan. Fluctuation theorem for stochastic dynamics. *J. Phys. A: Math. Gen.*, 31:3719, 1998.
- [5] G. E. Crooks. Nonequilibrium measurements of free energy differences for microscopically reversible markovian systems. *J. Stat. Phys.*, 90(5/6):1481–1487, 1998.
- [6] J. L. Lebowitz and H. Spohn. A Gallavotti-Cohen-type symmetry in the large deviation functional for stochastic dynamics. *J. Stat. Phys.*, 95:333, 1999.
- [7] D. Collin, F. Ritort, C. Jarzynski, S. B. Smith, I. Tinoco Jr., and C. Bustamante. Verification of the Crooks fluctuation theorem and recovery of RNA folding free energies. *Nature*, 437:231, 2005.
- [8] H. Leff and A. Rex. *Maxwell’s Demon 2: Entropy, Classical and Quantum Information, Computing*. Taylor and Francis, New York, 2002.
- [9] K. Maruyama, F. Nori, and V. Vedral. Colloquium: The physics of Maxwell’s demon and information. *2009*, 81:1, Rev. Mod. Phys.
- [10] M. v. Smoluchowski. Drei vorträge über diffusion, etc. *Physik. Zeit.*, XVII:557–571, 1916.
- [11] L. Szilard. On the decrease of entropy in a thermodynamic system by the intervention of intelligent beings. *Z. Phys.*, 53:840–856, 1929.
- [12] R. Landauer. Irreversibility and heat generation in the computing process. *IBM J. Res. Develop.*, 5(3):183–191, 1961.
- [13] O. Penrose. *Foundations of statistical mechanics; a deductive treatment*. Pergamon Press, Oxford, 1970.
- [14] C. H. Bennett. Thermodynamics of computation - a review. *Intl. J. Theo. Phys.*, 21:905, 1982.
- [15] A. Brut, A. Arakelyan, A. Petrosyan, S. Ciliberto, R. Dilenschneider, and E. Lutz. Experimental verification of landauers principle linking information and thermodynamics. *Nature*, 483:187, 2012.
- [16] A. B. Boyd and J. P. Crutchfield. Demon dynamics: Deterministic chaos, the Szilard map, and the intelligence of thermodynamic systems. 2015. SFI Working Paper 15-06-019; arxiv.org:1506.04327 [cond-mat.stat-mech].
- [17] S. Deffner and C. Jarzynski. Information processing and the second law of thermodynamics: An inclusive, Hamiltonian approach. *Phys. Rev. X*, 3:041003, 2013.
- [18] A. C. Barato and U. Seifert. Stochastic thermodynamics with information reservoirs. *Phys. Rev. E*, 90:042150, 2014.
- [19] T. M. Cover and J. A. Thomas. *Elements of Information Theory*. Wiley-Interscience, New York, second edition, 2006.
- [20] H. Touchette and S. Lloyd. Information-theoretic limits of control. *Phys. Rev. Lett.*, 84:1156, 2000.
- [21] F. J. Cao, L. Dinis, and J. M. R. Parrondo. Feedback control in a collective flashing ratchet. *Phys. Rev. Lett.*, 93:040603, 2004.
- [22] T. Sagawa and M. Ueda. Generalized Jarzynski equality under nonequilibrium feedback control. *Phys. Rev. Lett.*, 104:090602, 2010.
- [23] S. Toyabe, T. Sagawa, M. Ueda, E. Muneyuki, and M. Sano. Experimental demonstration of information-to-energy conversion and validation of the generalized Jarzynski equality. *Nature Physics*, 6:988–992, 2010.
- [24] M. Pomurugan. Generalized detailed fluctuation theorem under nonequilibrium feedback control. *Phys. Rev. E*, 82:031129, 2010.
- [25] J. M. Horowitz and S. Vaikuntanathan. Nonequilibrium detailed fluctuation theorem for repeated discrete feedback. *Phys. Rev. E*, 82:061120, 2010.
- [26] J. M. Horowitz and J. M. R. Parrondo. Thermodynamic reversibility in feedback processes. *Europhys. Lett.*, 95:10005, 2011.
- [27] L. Granger and H. Krantz. Thermodynamic cost of measurements. *Phys. Rev. E*, 84:061110, 2011.
- [28] D. Abreu and U. Seifert. Extracting work from a single heat bath through feedback. *Europhys. Lett.*, 94:10001, 2011.
- [29] S. Vaikuntanathan and C. Jarzynski. Modeling Maxwell’s demon with a microcanonical szilard engine. *Phys. Rev. E*, 83:061120, 2011.
- [30] A. Abreu and U. Seifert. Thermodynamics of genuine nonequilibrium states under feedback control. *Phys. Rev. Lett.*, 108:030601, 2012.
- [31] A. Kundu. Nonequilibrium fluctuation theorem for systems under discrete and continuous feedback control. *Phys. Rev. E*, 86:021107, 2012.
- [32] T. Sagawa and M. Ueda. Fluctuation theorem with information exchange: role of correlations in stochastic thermodynamics. *Phys. Rev. Lett.*, 109:180602, 2012.
- [33] L. B. Kish and C. G. Granqvist. Energy requirement of control: Comments on Szilard’s engine and Maxwell’s demon. *Europhys. Lett.*, 98:68001, 2012.
- [34] S. Ito and T. Sagawa. Information thermodynamics on causal networks. *Phys. Rev. Lett.*, 111:180603, 2013.
- [35] D. Hartich, A. C. A. C. Barato, and U. Seifert. Stochastic thermodynamics of bipartite systems: transfer entropy inequalities and a maxwell’s demon interpretation. *J. Stat. Mech.: Theor. Exp.*, 2013:P02016, 2014.
- [36] J. M. Horowitz and M. Esposito. Thermodynamics with continuous information flow. *Phys. Rev. X*, 4:031015, 2014.
- [37] J. M. Horowitz. Multipartite information flow for multiple Maxwell demons. *J. Stat. Mech.: Theor. Exp.*, 2015:P03006, 2015.
- [38] M. Esposito and G. Schaller. Stochastic thermodynam-

- ics for "Maxwell demon" feedbacks. *Europhys. Lett.*, 99:30003, 2012.
- [39] P. Strasberg, G. Schaller, T. Brandes, and M. Esposito. Thermodynamics of a physical model implementing a Maxwell demon. *Phys. Rev. Lett.*, 110:040601, 2013.
- [40] J. M. Horowitz, T. Sagawa, and J. M. R. Parrondo. Imitating chemical motors with optimal information motors. *Phys. Rev. Lett.*, 111:010602, 2013.
- [41] A. C. Barato and U. Seifert. Unifying three perspectives on information processing in stochastic thermodynamics. *Phys. Rev. Lett.*, 112:090601, 2014.
- [42] J. M. Horowitz and H. Sandberg. Second-law-like inequalities with information and their interpretations. *New J. Phys.*, 16:125007, 2014.
- [43] D. Mandal and C. Jarzynski. Work and information processing in a solvable model of Maxwell's demon. *Proc. Natl. Acad. Sci. USA*, 109(29):11641–11645, 2012.
- [44] D. Mandal, H. T. Quan, and C. Jarzynski. Maxwell's refrigerator: an exactly solvable model. *Phys. Rev. Lett.*, 111:030602, 2013.
- [45] A. C. Barato and U. Seifert. An autonomous and reversible Maxwell's demon. *Europhys. Lett.*, 101:60001, 2013.
- [46] J. Hoppenau and A. Engel. On the energetics of information exchange. *Europhys. Lett.*, 105:50002, 2014.
- [47] Z. Lu, D. Mandal, and C. Jarzynski. Engineering Maxwell's demon. *Physics Today*, 67(8):60–61, January 2014.
- [48] N. Merhav. Sequence complexity and work extraction. arXiv:1503.07653, 2015.
- [49] J. Um, H. Hinrichsen, C. Kwon, and H. Park. Total cost of operating an information engine. arXiv:1501.03733 [cond-mat.stat-mech], 2015.
- [50] J. R. Dorfman. *An Introduction to Chaos in Nonequilibrium Statistical Mechanics*. Cambridge University Press, Cambridge, United Kingdom, 1999.
- [51] B. Alberts, A. Johnson, J. Lewis, D. Morgan, and M. Raff. *Molecular Biology of the Cell*. Garland Science, New York, sixth edition, 2014.
- [52] H. R. Lewis and C. H. Papadimitriou. *Elements of the Theory of Computation*. Prentice-Hall, Englewood Cliffs, N.J., second edition, 1998.
- [53] P. Strasberg, J. Cerrillo, G. Schaller, and T. Brandes. Thermodynamics of stochastic Turing machines. arXiv:1506.00894, 2015.
- [54] C. Moore. Unpredictability and undecidability in dynamical systems. *Phys. Rev. Lett.*, 64:2354, 1990.
- [55] J. P. Crutchfield and D. P. Feldman. Regularities unseen, randomness observed: Levels of entropy convergence. *CHAOS*, 13(1):25–54, 2003.
- [56] *The Entropy of Functions of Finite-state Markov Chains*, volume 28, Publishing House of the Czechoslovak Academy of Sciences, Prague, 1957. Held at Liblice near Prague from November 28 to 30, 1956.
- [57] B. Marcus, K. Petersen, and T. Weissman, editors. *Entropy of Hidden Markov Process and Connections to Dynamical Systems*, volume 385 of *Lecture Notes Series*. London Mathematical Society, 2011.
- [58] P. M. Riechers and J. P. Crutchfield. Broken reversibility: Fluctuation theorems, path entropies, and exact results for complex nonequilibrium systems. *in preparation*, 2015.
- [59] N. Barnett and J. P. Crutchfield. Computational mechanics of input-output processes: Structured transformations and the  $\epsilon$ -transducer. *J. Stat. Phys.*, to appear, 2015. SFI Working Paper 14-12-046; arxiv.org: 1412.2690 [cond-mat.stat-mech].
- [60] C. E. Shannon. A mathematical theory of communication. *Bell Sys. Tech. J.*, 27:379–423, 623–656, 1948.
- [61] C. Jarzynski. Nonequilibrium equality for free energy differences. *Phys. Rev. Lett.*, 78(14):2690–2693, 1997.
- [62] J. P. Crutchfield. Between order and chaos. *Nature Physics*, 8(January):17–24, 2012.